Polymer Chemistry

Accepted Manuscript

ROYAL SOCIETY OF CHEMISTRY

www.rsc.org/polymers

RSCPublishing

ARTICLE

Dual-cure photochemical/thermal polymerization of acrylates: a photoassisted process at low light intensity

M. Retailleau, A. Ibrahim and X. Allonas*

Cite this: DOI: 10.1039/x0xx00000x

Received ooth January 2012,
Accepted ooth January 2012

DOI: 10.1039/x0xx00000x

www.rsc.org/

The dual-cure polymerization of an acrylate resin was investigated by combining a conventional technique (temperature measurement at the surface and in the deep) with confocal Raman microscopy. Polymerization was first characterized using a thermal initiator alone. Results showed that the thermal system polymerizes slowly and gradually, generating a thermal front that propagates from the bottom of the sample to the surface. Then, a photoinitiator was added to that thermal system. Unexpectedly, at the beginning of the reaction, the addition slows the thermal polymerization reaction. But quickly, the reaction is accelerated and an almost fully cured material is obtained in a shorter time than the net thermal system. This behaviour highlights a surprising synergistic effect between a photoinitiator and a thermal initiator in the dual-cure polymerization of thick materials.

Introduction

Photopolymerization has emerged as an inexpensive and efficient method for producing thin polymeric films and coatings. [1-3] The main shortcoming of this process lies in the limited penetration of UV radiation into organic materials. In a clear formulation, the incident light is mainly absorbed by the photoinitiator, which leads to a top to bottom gradient for the photogenerated initiating species, and also for the monomer conversion.[1-7]

Recently, photocuring production of thick polymers and composites has materialized.[8-11] Performing frontal polymerization makes possible the cure of thick polymers by means of UV light.[12] Frontal polymerization (FP) is a process in which a monomer is converted into a polymer via a localized reaction zone or propagating front.[13-15] Different process has been used to start fronts. The most common is to use a thermoelectric heater such as a soldering iron with peroxide as initiator.[16-18] Alternatively, a UV source can be applied if a photoinitiator is also present.[19] Frontal photopolymerization is utilized in diverse fabrication processes, ranging from photolithography of microcircuits to dental restorative and other biomedical materials, numerous coatings applications and microfluidic devices.[19-25]

Laboratory of Macromolecular Photochemistry and Engineering, University of Haute Alsace, 3b rue Alfred Werner, 68093 Mulhouse, France. E-mail: xavier.allonas@uha.fr; Fax: +33 389335014; Tel: +33 389335011

However, few studies interpret the effect of the photochemical contribution by using UV light as source to initiate the thermal front on the thermal polymerization reaction. Such a study appears to be a prerequisite to the creation of on-demand photoassisted thick polymers such as required in the field of composites.

In this paper, the polymerization of an acrylate resin was performed using either a thermal initiator, a photoinitiator or a combination of both. The polymerization is followed at the surface and in depth through the measurement of the evolved exotherm. Confocal Raman microscopy was used to follow the propagation of the polymerization reaction with time. The effect of the photopolymerization is clearly highlighted as resulting in the formation of a protective gel that permits a better maturation of the thermal process.

Materials and method

Formulation preparation

The resin used in this study was prepared by mixing Ebecryl 270 (E270, Cytec) with 50 wt % of tripropylene glycol diacrylate (SR306, Sartomer) for 5 min at 60-70 °C.

The examined thermal formulations were prepared by combining a thermal initiator *tert*-butyl hydroperoxyde (70 %) (TBH, Alfa Aesar) with Cobalt (II) 2-ethylhexanoate (Co^{II}), Sigma-Aldrich) as drier. The drier was added at 0.1 wt % to 14 g of the resin mixture, while the addition of the

hydroperoxide takes place just before measurement. The polymerization reaction was performed under air at room temperature on 13 mm thick samples (silicon mold, truncated cone shape, h = 15 mm, r_{inf} = 31 mm and r_{sup} = 42 mm).
Diphenyl(2,4,6-trimethylbenzoyl)-phosphine oxide (TPO, Sigma-Aldrich) was used as Type I photoinitiator at a concentration of 0.1 wt %. The surface of the sample was irradiated homogeneously using a high pressure mercury-xenon lamp (Hamamatsu) equipped with a reflector at 365 nm and coupled with a flexible light-guide. An additional optical interference filter at 365 nm was used to select the wavelength. The irradiation start time was fixed at 30 min after the addition of TBH to the formulation for 60 s with an intensity of 2 mW.cm^{-2} at the sample surface.

Temperature measurement

The time evolution of the temperature is directly proportional to the rate of conversion and gives an indirect measurement of the polymerization reaction, assuming no heat loss.[26] For our experiments, the temperature was measured by a thermocouple at a depth of 10 mm, and by an optical pyrometer (OP) at the surface of the sample. The type K thermocouple, electrically insulated from the mixture with a PFA Teflon, was connected to a portable data logger (OM-DAQPRO-5300, Omega Engineering, Inc., Stamford, CT), that was set at a recording frequency of 1 Hz. A Omega OS550A Industrial Infrared Thermometer (Omega Engineering, Inc., Stamford, CT) equipped with a laser-sighting device (OS550-LS) was used as optical pyrometer. This instrument shows a sensitivity of 1 °C with an operating range of -23 to 538 °C. The distance between the OP sensor and the sample surface was 15.2 cm with a 3.9 mm focal spot diameter. The instrument was set to acquire temperatures at a frequency of 1 Hz with an emissivity coefficient of 0.95.
Optical pyrometry was developed by Crivello [26] as an analytical technique for continuous monitoring of the progress of both free-radical and cationic photopolymerizations. This technique provides fast and reproducible results for micrometer(s)-thick samples. As our sample is 13 mm thick, the temperature measured by the OP will be considered as the surface temperature. The temperature profiles obtained by both techniques allow the characterization of the polymerization by the extraction of the following parameters (Figure 1): the maximal temperature (T_{max}), the time required to reach T_{max} (t_{Tmax}) and the temperature jump due the heat evolved by the reaction ($\Delta T = T_{max} - T_{initial}$).

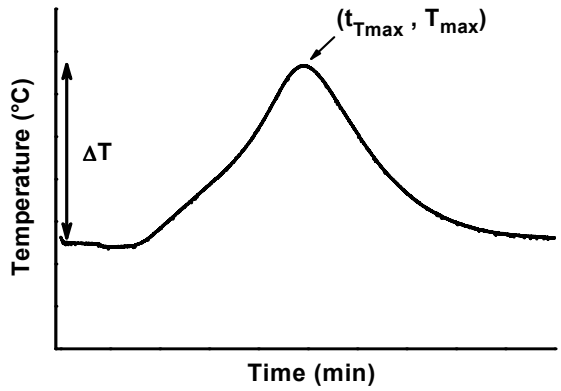

Figure 1 - Definition of the parameter: T_{max}, t_{Tmax} and ΔT

Confocal Raman microscopy

Confocal Raman microscopy (CRM) enables the recording of Raman spectra at different depths into a sample by focusing the exciting laser light at different positions. Measurements were performed on an inVia Reflex Raman microscope from Renishaw which is a combination of a Raman spectrometer and a Leica DM2500 microscope.[27, 28] The probe wavelength was provided by a helium–neon laser from Renishaw emitting 17 mW.cm^{-2} at 633 nm. It was verified that this wavelength did not imply any postcuring on the sample during CRM measurements. 10 s of accumulation were needed at each step to obtain a reasonable signal-to-noise ratio in buried layers. A circular polarization of the laser beam was achieved by placing a λ/4 waveplate in the optical path of the incident light to eliminate polarization effects. Two dielectric rejection filters were used to prevent the backscattered light from the laser from entering the spectrophotometer. A 600 l.mm^{-1} grating optimized for the visible light and providing a spectral window of 1950 cm^{-1} was used to disperse the light on a charge-coupled device (CCD) NIR deep depletion Peltier cooled detector camera. The confocal mode was defined by the spectrophotometer entrance slit opened to 20 µm in the back focal plane of the objective lens and a selection of 3 pixels perpendicular to the slit axis on the CCD camera. The spectral resolution given by the combination slit/CCD/grating was 7.1 cm^{-1}. A dry objective (N PLAN 50×) from Leica, with a numerical aperture of 0.5 and a working distance of 8.2 mm was chosen to perform depth profiling of the cured layers. In these conditions, the depth resolution ($\approx 4 * \lambda/ON^2$) and the radial resolution ($\approx 4 * \lambda/ON$) were 1 and 0.5 µm, respectively. Due to the use of a dry objective, the nominal depth does not represent the real depth of the sample.[29] Samples having the same thickness are then compared as a function of the nominal depth.[30]
Depth conversion profiles (nominal displacement of the optical plate holding the sample) were plotted at different time. The area of the νC=C vibration band ($A_{\nu C=C}$) at 1636 cm^{-1} was followed as a function of the depth and the area of the γC-H

vibration band ($A_{\gamma C\text{-}H}$) at 779 cm^{-1} from the isophorone ring of the Ebecryl 270 which was not affected by the curing process, was used as reference to normalize the νC=C vibration band. The conversion as a function of depth was then calculated as follow:

$$Conv_{Raman} = 100 * (1 - A_z/A_m) \quad (1)$$

With $A_z = (A_{\nu C=C}/A_{\gamma C-H})_z$ at a given depth z and $A_m = (A_{\nu C=C}/A_{\gamma C-H})_m$ determined from the liquid formulation scanned in the same experimental conditions as for the cured sample.

UV-visible spectrometer

Absorbance spectra of solutions were recorded on A Cary 4000 UV–Visible Spectrophotometer (Varian). These experiments were performed in ethanol using 1 cm quartz cell.

Results and discussions

Thermal system

Impact of TBH concentration

The peroxide/cobalt initiating system is widely used in industry to start the free radical polymerization of unsaturated resins. Cobalt salts are well known as peroxide decomposers and this leads to the formation of initiating radicals. Due to oxygen inhibition, which is predominant at the surface, the reaction starts preferentially in depth. All experiments were performed at room temperature.[31]

For initiating systems based on a cobalt salt and a peroxide, the use of cobalt as drier is limited to low concentrations (0.05 wt % to 0.2 wt %) to prevent premature curing of the surface and excessive coloring.[31] The resulting polymerization, referred as bulk polymerization, is exothermic and its efficiency is thus depending on the peroxide amount. The effect of TBH amount (0.2 to 3 wt %) was studied by following the temperature profiles at the surface and in deep zones by using the thermocouple/OP device. As example, Figure 2 shows the measured temperature profiles of samples prepared with 1 wt % and 3 wt % of TBH.

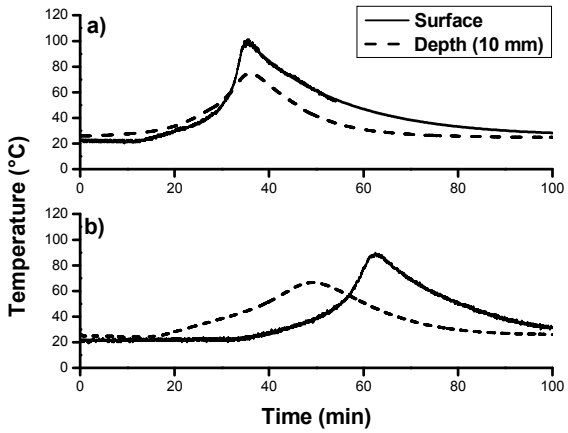

Figure 2 - Temperature profile obtained with the thermocouple-OP device a) 3 wt % TBH, b) 1 wt % TBH

As can be seen, homogeneous temperature profiles with comparable t_{Tmax} values were obtained for the formulation prepared with 3 wt % of TBH. Although, the temperature of the surface was 30 °C higher than the one measured in the deep.

By decreasing TBH amount, the measured temperature profiles noticeably differentiates with a shorter t_{Tmax} value in the deep comparing to the one obtained at the surface with the OP. These results show that the evolution of the temperature profiles through the thickness depends on the peroxide concentration. To clarify this effect, the evolution of ΔT and t_{Tmax} values versus TBH amount is plotted in Figure 3. This figure shows comparable ΔT profiles and t_{Tmax} evolution at the surface and in the deep. Experiments carried out with 0.2 wt % of TBH are not shown, as they did not exhibit noticeable exothermic peak even if a part of the formulation was polymerized.

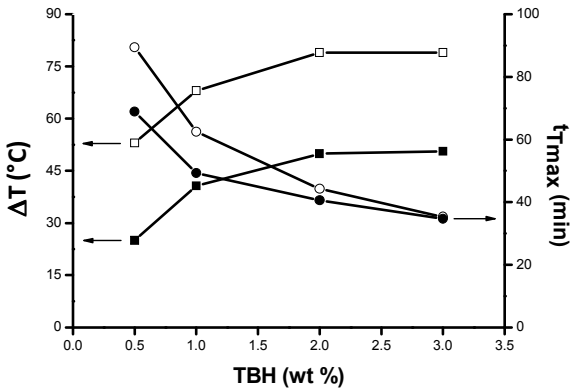

Figure 3 - Influence of TBH concentration (from 0.5 to 3 wt %) on ΔT (squares) and t_{Tmax} (circles) respectively at the surface (open symbols) and in the deep (filled symbols).

As can be seen, the time required to reach the maximal temperature increases with decreasing the TBH concentration. This can be explained by the corresponding decrease in

initiating radicals which slows down the reaction. In addition, the t_{Tmax} values measured at the surface are higher than those measured in the deep for low concentration of TBH. From these results, one can conclude that the reaction starts in the deep area after full consumption of the dissolved oxygen by the initiating radicals. A retarding effect is observed at the surface where oxygen is continuously replenished from the atmosphere until the thermal front generated in depth propagates from the bulk to the surface. From that point of view, there is an analogy with frontal polymerization.[13, 32] Moreover, the difference calculated between the value of t_{Tmax} at the surface and in the deep for each TBH amount shows a decreasing from 13 min at 1 wt % to 0.5 min at 3 wt % indicating that the thermal front propagates faster at high TBH concentration. Regarding the ΔT values evolution at the surface and in the deep, an increase was observed with increasing TBH amount related to the increase of the available initiating radicals. The ΔT values reach a plateau for a TBH amount higher than 2 wt %.

In addition, the temperature at the surface and in the deep show a constant difference around 30 °C. This difference could be explained by a change in both viscosity of the resin and the corresponding thermal diffusivity coefficient through the thickness caused by the propagation of the the thermal front.[33, 34] Based on these results, it was found that the time evolution of the temperature (and subsequently of the polymerization reaction) is not homogeneous through the sample thickness and depends on the amount of peroxide. This deserves a more detailed study by confocal Raman microscopy.

Monitoring thermal curing by Raman confocal microscopy

To have more insight into the influence of TBH concentration on the conversion, depth profiles were carried out at different curing time (from 1 to 30 h) with increasing TBH concentrations (from 0.2 wt % to 3 wt %) by using confocal Raman microscopy. For high amount of TBH (higher than 2 wt %), an efficient polymerization reaction takes place as confirmed by the fast propagation of the thermal front. This is confirmed by the depth profiles obtained by the CRM which show that almost 93 % of conversion is obtained in less than 1 h. By contrast, for low amount of TBH, the temperature profiles are different in the bulk and at the surface, a fact which in turn leads to interesting time evolution of the depth conversion profiles as shown in Figure 4 (see ESI).

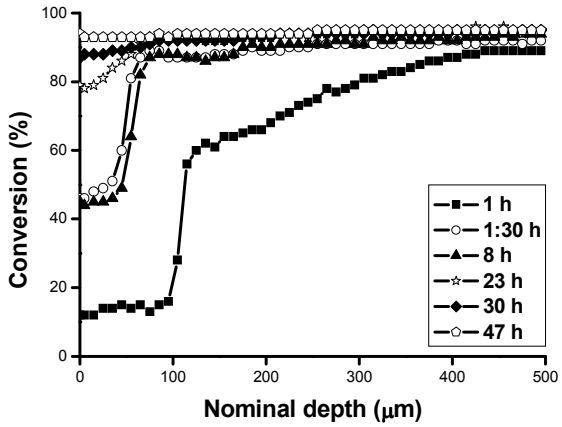

Figure 4 - Depth conversion profile of the polymer (E270/SR306; 0.2 wt % Co^{II}; 1 wt % TBH) at different curing time.

As can be seen, the polymerization reaction is not complete after 1 h and a 100 μm thick inhibited layer can be observed. A decrease of the inhibited layer up to 40 μm and an increase of the conversion percentage to 85 % were observed after a reaction time of 1:30 h. Then, the conversion profile is stable at least 8 h indicating a slow polymerization process. These results are in line with the measured temperature profile of this sample (Figure 2) showing that the sample already cooled down to room temperature after 1:40 h. Buoyancy-driven convection was ruled out for two main reasons: a/ in the areas where the polymerization process takes place, more than 50% of monomer conversion is obtained, preventing any further mass transport in the medium; b) all the samples exhibited a homogeneous conversion in the XY plane and only inhomogeneous conversion along the Z plane.

Nonetheless, the polymerization reaction at the surface continues slowly due to the diffusion of macroradicals. Finally, after 47 h, the reaction was complete with a conversion of about 95 %.

From these results, one can conclude that the surface was not fully cured compared to the deep at short reaction time (about 1 h) due to the oxygen inhibition of the radicals.[27, 35] Moreover, the presence of monomer conversion gradient through the thickness was noticed, confirming the formation of a thermal front in the deep zones and its slow propagation to the surface.

Impact of TBH concentration

In order to have more information concerning the impact of TBH amount, the conversion profiles (for the first 500 μm) were plotted for different TBH concentrations (Figure 5).

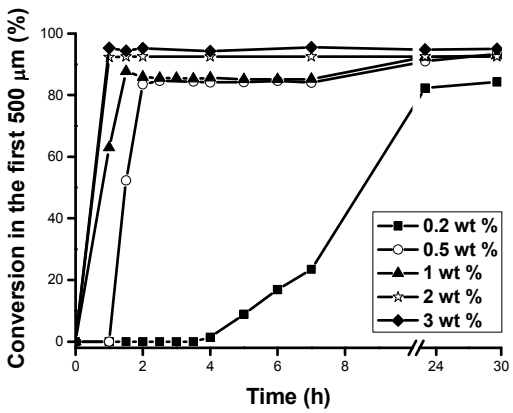

Figure 5 - Time evolution of the conversion for different TBH concentrations (from 0.5 to 3 wt %).

As presented in Figure 3, the formulation prepared with 0.2 wt % TBH shows the higher t_{Tmax} value indicating that slow polymerization reaction take places. The evolution of the conversion with time over the first 500 µm (Figure 5) supports these results: four hours were necessary to start the reaction at the surface. This behaviour is in agreement with the temperature profiles measured for this sample where the heat evolvement did not induce an increase of the temperature (thermalization of the sample). After 4 hours, a slow decrease of the inhibited layer was noticed. Even after a reaction time around 30 hours, the presence of a small inhibited layer (50 µm) was observed. With 0.5 wt % of TBH, a time shorter than 2 hours was sufficient to reach a conversion of 85% with a residual inhibited layer of 60 µm. The reaction also started in the deep areas, but the initial concentration of reactive species is higher, leading to the formation of a propagating thermal front from the deep to the surface of the sample. With this front will be evolved a sufficient temperature to auto-accelerate the cobalt/peroxide reaction that leads to the formation of radicals. The thermal front propagation speed and subsequently the time necessary to induce a complete polymerization of the sample depend primarily on the initial concentration of initiating species formed on the deep zone related to the TBH concentration. Thus, CRM results confirm the hypothesis indicating the presence of a thermal front where its speed is related to the TBH amount.

Photochemical system

In order to accelerate and ensure control of the polymerization reaction at the surface, a photoinitiator was added to the formulation. In the presence of a photoinitiator, one can postulate that the irradiation will initiate the polymerization reaction at the surface, ensuring the formation of a second thermal front that will propagates from the surface to the deep zones. The propagation of this photoinitiated thermal front will promote the cobalt/peroxide auto-oxidation reaction. The propagation of two thermal fronts in opposite directions through the sample will be expected.

Before studying the performance of the combined photochemical-thermal system, it is worth to investigate the effect of photochemical process alone, i.e. without any thermal initiator. The obtained depth profiles at different reaction time (from 1 to 30 h) and the associated temperature profile are presented in Figure 6.

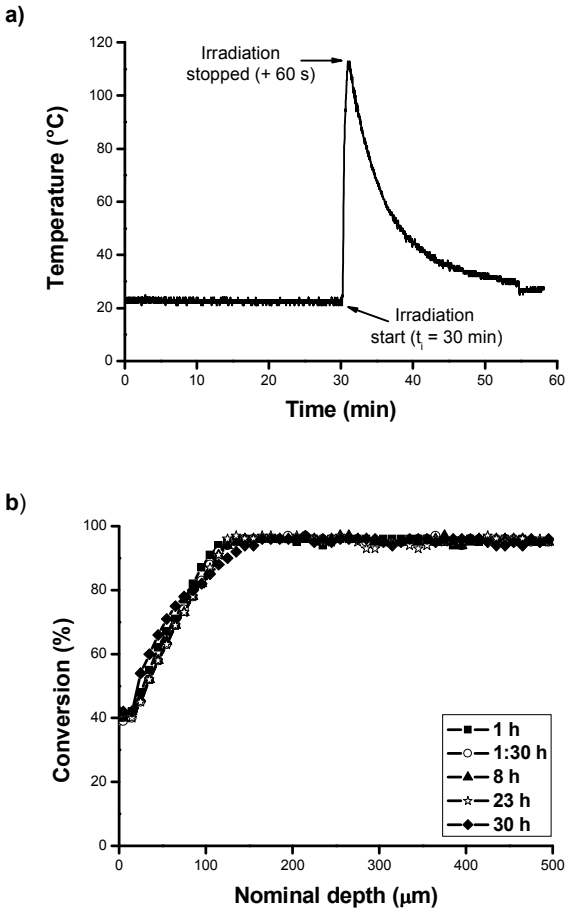

Figure 6 - Photopolymerization reaction probed a) from the surface temperature and b) from the depth conversion profiles (0.1 wt% TPO).

The temperature profile obtained by OP technique (Figure 6a) showed a temperature increase coinciding with the irradiation start. A maximal value around 112 °C was reached when the irradiation was stopped. After turning off the UV irradiation, immediate decrease of the temperature was observed up to thermalization at room temperature after 30 minutes. This temperature profile supports the proposal that the irradiation allows the control of the initiation process of the polymerization reaction at the surface.

TPO concentration and irradiation intensity (2 mW/cm²) were chosen in order to avoid deformation of the surface as can be observed at higher values. The depth profiles (Figure 6b) exhibited a small inhibited layer around 30 µm and a high conversion value of about 88.5 % after 1 h. However, the depth profile remains stable over the reaction time indicating the

absence of dark polymerization reaction. Moreover, the low concentration of TPO and low intensity limits the penetration of the light over the sample. As a consequence, only 3 mm thick sample can be cured by light.

During photopolymerization reaction, a high temperature (112 °C) was reached at the surface which could enable to trigger the cobalt/peroxide reaction in a photo-thermal system.

Photo-thermal system

According to previous results, one can imagine that combining both thermal and photochemical systems could enhance the system efficiency: TPO could cure the surface (fast process); TBH/Co^{II} can cure the deep (slow and continuous process).

In an attempt to ascertain the previous hypothesis, 0.1 wt % of TPO was added to the thermal system containing 0.1 and 1 wt % of Co^{II} and TBH, respectively. To get the full effect of the two polymerization processes, the sample irradiation was started 30 min after the addition of TBH, giving time to the thermal polymerization to start (Figure 2b).

Depth profiles for this sample were recorded with the CRM at different reaction times (from 1 to 30 h) as shown in Figure 7.

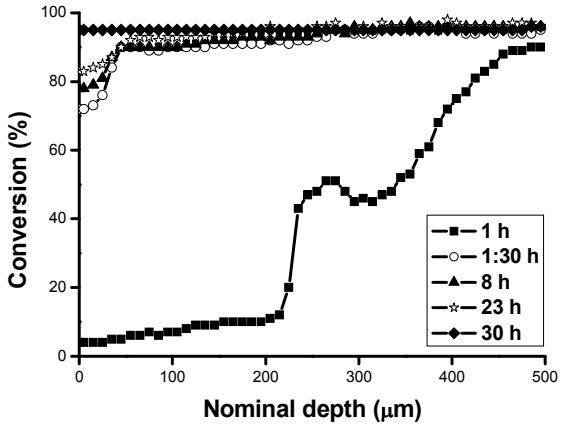

Figure 7 - Time evolution of the depth conversion profiles obtained through photo-thermal initiation process (0.1 wt % TPO; 0.2 wt % Co^{II}; 1 wt % TBH).

In the first 500 µm of the surface sample, the polymerization reaction is not complete after 1 hour. Indeed, a mean conversion of 36% was obtained by summing the CRM results over a 500µm-domain and a 220 µm thick inhibited layer is noticed. Interestingly, these values show that the combined photo-thermal system shows low performance comparing to that observed for the thermal and photochemical systems after 1 hour reaction time. However, quite surprisingly, few more minutes (*i.e.* 1:30 h reaction time) were sufficient to achieve a highly efficient polymerization with conversion and inhibited layer around 95 % and 20 µm respectively. From these results, particular reaction behaviour was observed for the photo-thermal system during the first 90 minutes time reaction: first a slow polymerization process occurs during the first hour of the reaction followed by fast improvement of the efficiency within the next 30 minutes.

An attempt was made to understand the slow polymerization reaction observed during the first hour of reaction when using the photo-thermal process. This effect may be attributed to an internal filter effect due to the presence of Co^{II} and TBH that may decrease the intensity of light absorbed by TPO at the considered wavelength (365 nm). Figure 8 shows the absorption spectra of TPO, Co^{II}, TBH and TBH/Co^{II} combination measured in ethanol at the same concentrations than in the formulations.

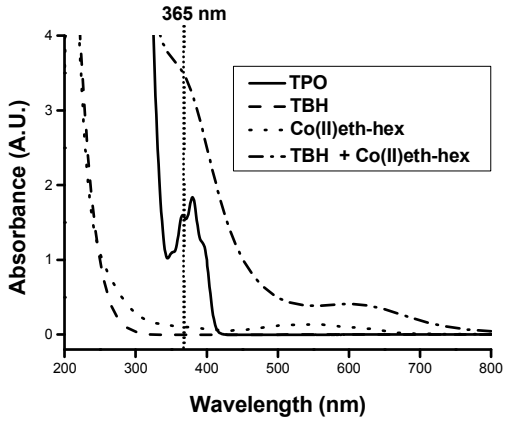

Figure 8 - Absorption spectrum of TPO (3.19 10^{-3} mol/L), TBH (0.121 mol/L), Co^{II} : 6.42 10^{-3} mol/L and a TBH/Co^{II} mixture (0.121 mol/L/6.42 10^{-3} mol/L)

As can be seen, Co^{II} and TBH do not absorb significantly at 365 nm at these concentrations and, moreover, these individual components do not change the absorption spectrum of TPO in physical mixture (results not shown here). However, a change in absorption spectra was observed when mixing Co^{II} with TBH, which could be attributed to the coordination complex formed between TBH and the Co^{II} ion.[36] Under these experimental conditions, the absorbance of the Co^{II}/TBH complex exceeds by a factor of 3 the one of TPO at 365 nm, a fact which obviously explains the decrease in the photochemical process.

As said before, after a first slowing down of the reaction, a clear acceleration of the polymerization reaction occurs after 60 minutes, as confirmed by the temperature profiles at the surface (Figure 9).

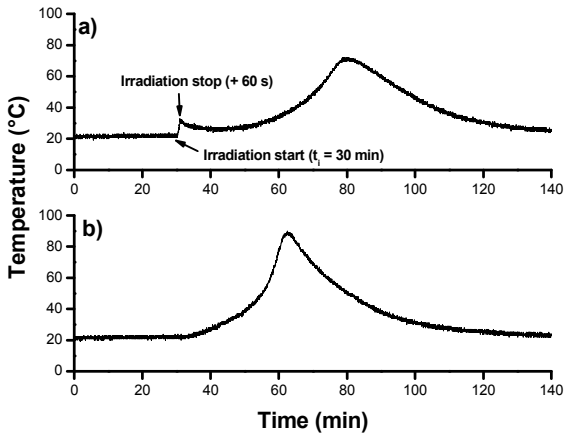

Figure 9 - Time evolution of the surface temperature for a) photo-thermal system (0.1 wt % TPO; 0.2 wt % Co^{II}; 1 wt % TBH) and b) thermal system (0.2 wt % Co^{II}; 1 wt % TBH).

The temperature profile measured at the surface showed two exothermic peaks. The beginning of the first peak coincides with the irradiation start. A low ΔT value of 10 °C was reached at the end of the irradiation which was 80 °C lower than the one obtained with the net photochemical system. This result support the internal filter effect discussed above. After turning off the UV irradiation, immediate decrease of the temperature was observed which stabilized during 10 min at 27 °C. This indicates that the initiating TPO photopolymerization reaction does not produce enough energy to initiate the propagation of polymerization front from the surface to the bottom of the sample. Nevertheless, after this lead time, a second exothermic peak started to appear at a reaction time of 60 min and reaches a temperature of 71 °C at 90 min, as a consequence of the thermal front progress. This exotherm appears to be 20 °C lower than that obtained with the net thermal system and t_{Tmax} is delayed by 17 min. This shape with two exothermic peaks can explain the particular conversion profile observed with CRM recorded at 1 h: indeed, Figure 7 shows the appearance of a conversion peak between 220 µm and 310 µm superimposed to a more conventional depth profile which could be attributed to the TPO photoinitiated polymerization reaction (see ESI for reproducibility experiment). In this area, the 50 % of conversion obtained photochemically allows the formation of a gel of high viscosity located slightly below the surface which in turn will limit the diffusion of O_2. Thus, the photopolymerization event leads to the formation of a barrier against oxygen diffusion.

This photochemically induced gelified layer protects the deeper layers from the diffusion of oxygen. Therefore, when the thermal front appears after 60 min, an acceleration of the process can be noticed. A decrease of the inhibited layer down to 20 µm and an increase of the conversion up to 90 % are reached after a reaction time of 1 h 30 (Figure 7). In addition, it could be seen from Figure 9 that the thermal front propagating from the bottom is detected at the surface with a 17 min delay, a fact that may be attributed to a difference of viscosity and thermal diffusivity in the photochemically induced gelified layer. Finally, after 30 h, the reaction was complete with a conversion around 95 %.

Conclusion

Herein, the polymerization reaction was studied by two techniques usually not combined which turned to be complementary: OP-thermocouple and confocal Raman microscopy. It is proposed that the thermal polymerization generates a thermal front in depth, propagating from the bulk to the surface. The addition of a photoinitiator to that thermal system showed an unexpected behaviour. It is suggested that, at low intensity and low photoinitiator concentration, a gel of high viscosity is generated slightly below the surface. This photochemically induced gelified layer protects the deeper layers from the diffusion of oxygen and permits a better maturation of the thermal process. This behavior highlights a surprising synergistic effect between a photoinitiator and a thermal initiator in the dual-cure polymerization of thick materials.

Acknowledgements

The authors thank Région Alsace, ADEME and Investissements d'Avenir for financial support. The French National Agency for Research (ANR) is also fully acknowledged for supporting the DeepCURE project.

Notes and references

1. J. G. Drobny, *Radiation Technology for Polymers*, Taylor & Francis, 2002.
2. R. Schwalm, *UV Coatings: Basics, Recent Developments and New Applications*, Elsevier Science, 2006.
3. X. Allonas, C. Croutxé-Barghorn, K. W. Bögl, N. Helle and G. A. Schreiber, in *Ullmann's Encyclopedia of Industrial Chemistry*, Wiley-VCH Verlag GmbH & Co. KGaA, 2000.
4. X. Allonas, C. Croutxe-Barghorn, J. P. Fouassier, J. Lalevee, J. P. Malval and F. Morlet-Savary, in *Lasers in Chemistry. Influencing Matter*, ed. M. Lackner, Wiley, Weinheim, 2008, vol. 2, ch. 35, p. 1001.
5. W. A. Green, *Industrial Photoinitiators: A Technical Guide*, CRC PressINC, 2010.
6. B. L. Rytov, V. B. Ivanov, V. V. Ivanov and V. M. Anisimov, *Polymer*, 1996, **37**, 5695-5698.
7. C. Decker, *Prog. Polym. Sci.*, 1996, **21**, 593-650.
8. V. Narayanan and A. B. Scranton, *Trends Polym. Sci.*, 1997, **5**, 415-419.
9. K. K. Baikerikar and A. B. Scranton, *Polymer*, 2001, **42**, 431-441.
10. K. K. Baikerikar and A. B. Scranton, *J. Appl. Polym. Sci.*, 2001, **81**, 3449-3461.
11. S. Gregory, Ultraviolet curable resin compositions having enhanced shadow cure properties, 2001, US Patent 6,245,827.
12. Y. Cui, J. Yang, Z. Zeng, Z. Zeng and Y. Chen, *Eur. Polym. J.*, 2007, **43**, 3912-3922.

13. J. A. Pojman, V. M. Ilyashenko and A. M. Khan, *J. Chem. Soc., Faraday Trans.*, 1996, **92**, 2825-2837.
14. J. A. Pojman, in *Polymer Science: A Comprehensive Reference*, eds. K. Matyjaszewski and M. Möller, Elsevier, Amsterdam, 2012, pp. 957-980.
15. A. Morales and J. A. Pojman, *J. Polym. Sci., Part A: Polym. Chem.*, 2013, **51**, 3850-3855.
16. N. M. Chechilo, R. J. Khvilivitskii and N. S. Enikolopyan, *Dokl. Akad. Nauk SSSR*, 1972, **204**, 1180-1181.
17. S. P. Davtyan, V. Z. Pavel and S. A. Vol'fson, *Russ. Chem. Rev.*, 1984, **53**, 150.
18. A. M. Khan and J. A. Pojman, *Trends Polym. Sci.*, 1996, **4**, 253-257.
19. C. Nason, T. Roper, C. Hoyle and J. A. Pojman, *Macromolecules*, 2005, **38**, 5506-5512.
20. J. T. Cabral, S. D. Hudson, C. Harrison and J. F. Douglas, *Langmuir*, 2004, **20**, 10020-10029.
21. C. Decker, *Polym. Int.*, 1998, **45**, 133-141.
22. C. Decker, *Polym. Int.*, 2002, **51**, 1141-1150.
23. H. Christopher, T. C. João, M. S. Christopher, K. Alamgir and J. A. Eric, *J. Micromech. Microeng.*, 2004, **14**, 153.
24. T. Wu, Y. Mei, J. T. Cabral, C. Xu and K. L. Beers, *J. Am. Chem. Soc.*, 2004, **126**, 9880-9881.
25. Z. T. Cygan, J. T. Cabral, K. L. Beers and E. J. Amis, *Langmuir*, 2005, **21**, 3629-3634.
26. B. Falk, S. M. Vallinas and J. V. Crivello, *J. Polym. Sci., Part A: Polym. Chem.*, 2003, **41**, 579-596.
27. F. Courtecuisse, J. Cerezo, C. Croutxé-Barghorn, C. Dietlin and X. Allonas, *J. Polym. Sci., Part A: Polym. Chem.*, 2013, **51**, 635-643.
28. F. Courtecuisse, A. Belbakra, C. Croutxé-Barghorn, X. Allonas and C. Dietlin, *J. Polym. Sci., Part A: Polym. Chem.*, 2011, **49**, 5169-5175.
29. F. Courtecuisse, C. Dietlin, C. Croutxé-Barghorn and L. G. J. Van Der Ven, in *Appl. Spectrosc.*, OSA, 2011, vol. 65, pp. 1126-1132.
30. R. Pynaert, J. Buguet, C. Croutxe-Barghorn, P. Moireau and X. Allonas, *Polym. Chem.*, 2013, **4**, 2475-2479.
31. M. D. Soucek, T. Khattab and J. Wu, *Prog. Org. Coat.*, 2012, **73**, 435-454.
32. V. A. Volpert, in *Advances in Sensing with Security Applications*, eds. A. Golovin and A. Nepomnyashchy, Springer Netherlands, 2006, vol. 218, ch. 07, pp. 195-245.
33. P. Martinez-Torres, A. Mandelis and J. J. Alvarado-Gil, *J. Appl. Phys.*, 2010, **108**, 054902-054902-054910.
34. H. Yu, Y. Fang, L. Chen and S. Chen, *Polym. Int.*, 2009, **58**, 851-857.
35. C. Decker and A. D. Jenkins, *Macromolecules*, 1985, **18**, 1241-1244.
36. N. Turrà, U. Neuenschwander, A. Baiker, J. Peeters and I. Hermans, *Chem. Eur. J.*, 2010, **16**, 13226-13235.